Resonant Rydberg Dressing of Alkaline-Earth Atoms via Electromagnetically Induced Transparency

C. Gaul, B. J. DeSalvo, J. A. Aman, F. B. Dunning, T. C. Killian, and T. Pohl

Resonant Rydberg-dressing of Alkaline-Earth Atoms via Electromagnetically Induced Transparency

C. Gaul,[1] B. J. DeSalvo,[2] J. A. Aman,[2] F. B. Dunning,[2] T. C. Killian,[2] and T. Pohl[1]

[1] *Max-Planck Institute for the Physics of Complex Systems, Nöthnitzer Str. 38, 01187 Dresden, Germany*
[2] *Rice University, Department of Physics and Astronomy and Rice Center for Quantum Materials, Houston, Texas 77251, USA*
(Dated: May 13, 2016)

We develop an approach to generate finite-range atomic interactions via optical Rydberg-state excitation and study the underlying excitation dynamics in theory and experiment. In contrast to previous work, the proposed scheme is based on resonant optical driving and the establishment of a dark state under conditions of electromagnetically induced transparency. Analyzing the driven dissipative dynamics of the atomic gas, we show that the interplay between coherent light coupling, radiative decay and strong Rydberg-Rydberg atom interactions leads to the emergence of sizeable effective interactions while providing remarkably long coherence times. The latter are studied experimentally in a cold gas of Strontium atoms for which the proposed scheme is most efficient. Our measured atom loss is in excellent agreement with the theoretical prediction based on binary effective interactions between the driven atoms.

Ultracold gases of interacting atoms provide powerful settings for exploring many-body physics in and out of equilibrium with a high level of control and experimental accessibility [1]. While most experiments exploit zero-range collisional interactions between atoms, the realization of finite range interactions would open up a whole new range of study and presents an exciting frontier in the field. Among currently pursued avenues are dipolar quantum gases composed of polar molecules [2–4] or atoms with large magnetic dipoles [5–7], laser-cooled ion crystals [8–11] and atoms in highly excited Rydberg states [12].

Owing to their large electronic orbit, Rydberg atoms feature very strong van der Waals interactions making them virtually ideal candidates for quantum simulations of spin models [13–16]. Yet, their radiative decay sets stringent limits on achievable coherence times, which thus far prevented the observation of long-time excitation dynamics or coherent interaction effects on atomic motion. Weak off-resonant excitation of Rydberg states has been proposed [17–21] as a solution to this problem. Working with only a small fraction of excited atoms, this so-called Rydberg dressing promises enhanced lifetimes while providing sizeable interactions. Such interactions have recently been observed in experiments with two trapped atoms [22], and are attracting broad interest in the context of quantum computing [23–25], frequency metrology [17, 26] as well as many-body physics in quantum gases [27–33] and synthetic quantum magnets [34–36] of Rydberg-dressed atoms. Yet, the generation of sufficiently strong interactions for such applications requires large light-atom coupling strengths that are challenging to achieve, in particular for two-photon excitation of alkali atoms as employed in most current experiments.

In this work, we describe a new approach to Rydberg dressing via *resonant* two-photon excitation of alkaline-earth atoms, which feature long-lived intermediate states and have recently become available to cold Rydberg gas
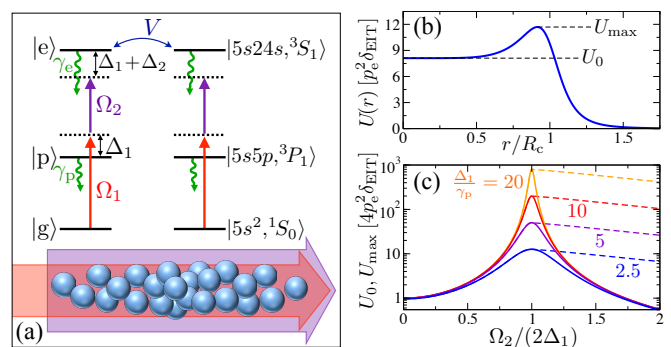

FIG. 1. (color online) (a) A gas of atoms is illuminated by two laser fields that drive a two-photon transition to a Rydberg level $|e\rangle$ with corresponding Rabi frequencies $\Omega_{1(2)}$ and detunings Δ_1 and Δ_2 of the lower and upper transition . The labels on the right indicate the states of Sr atoms employed in our experiments. Rydberg interactions, V, lead to an effective interaction potential between dressed atoms, shown in (b) for $\Delta_1/\gamma_{\rm p} = 2.5$, $\Omega_2/\Delta_1 = 2.3$ and $\gamma_{\rm e} = 0$. (d) Dependence of the characteristic energy scales U_0 (solid lines) and $U_{\rm max}$ (dashed lines) on Ω_2 and $\gamma_{\rm p}$.

experiments [37–40]. The underlying idea is based on the establishment of an approximate dark state with a strongly suppressed Rydberg state component and its modification by the mutual interactions between Rydberg atoms. We obtain a systematic solution of the N-body steady state in the limit of weak Rydberg excitation to show that this interplay gives rise to sizeable effective interactions between the driven atoms. In particular, we identify a two-body resonance that enables a high degree of interaction control and yields enhanced interactions at long coherence times. We experimentally realize two-photon Rydberg excitation via a long-lived triplet state of cold Strontium atoms and probe decoherence due to Rydberg-dressing by monitoring the induced atom loss. Our measured loss spectra reveal strong interaction effects and are in good agreement with the developed the-

ory based on emergent binary effective interactions.

We consider a gas with a density ρ_a composed of N three-level atoms at positions $\mathbf{r}_i$, $i = 1, ..., N$. At low temperatures, atomic motion is much slower than typical timescales of the internal state dynamics, such that we can focus on the latter within a Born-Oppenheimer approximation [18]. The ground state ($|g_i\rangle$) of the ith atom is coupled to an intermediate state ($|p_i\rangle$) with a Rabi frequency Ω_1 and frequency detuning Δ_1 [cf. Fig. 1(a)]. A second laser field drives the transition between $|p_i\rangle$ and a high lying Rydberg state ($|e_i\rangle$) with Ω_2 and a total frequency detuning of $\Delta_1 + \Delta_2$. The associated Hamiltonian for each atom can be written as

$$\hat{H}^{(i)} = \frac{\Omega_1^{(i)}}{2}\left(\hat{\sigma}_{gp}^{(i)} + \hat{\sigma}_{pg}^{(i)}\right) + \frac{\Omega_2^{(i)}}{2}\left(\hat{\sigma}_{ep}^{(i)} + \hat{\sigma}_{pe}^{(i)}\right)$$
$$- \Delta_1\hat{\sigma}_{pp}^{(i)} - (\Delta_1 + \Delta_2)\hat{\sigma}_{ee}^{(i)}, \qquad (1)$$

where $\hat{\sigma}_{\alpha\beta}^{(i)} = |\alpha_i\rangle\langle\beta_i|$ ($\alpha, \beta = $ g, p, e). In addition, the internal state dynamics is governed by single-particle dissipation described by Lindblad operators $\mathcal{L}_i(\hat{\rho})$ acting on the N-body density matrix $\hat{\rho}$ of the system. For now we include spontaneous decay of the intermediate and Rydberg state, with a rate γ_p and γ_e, respectively [cf. Fig. 1(a)]. In the absence of interactions the steady state of the corresponding Master equation factorizes into one-body states $\hat{\rho}_i^{(1)} = \mathrm{Tr}_{\bar{i}}\hat{\rho}$, where the subscript $\bar{i}$ denotes the trace over all but the ith atom. On two-photon resonance, $\Delta_1 + \Delta_2 = 0$, and for negligible Rydberg state decay it assumes the particularly simple form $\hat{\rho}_i^{(1)} = |d_i\rangle\langle d_i|$ of a dark state $|d_i\rangle \propto \Omega_2|g_i\rangle - \Omega_1|e_i\rangle$ [41]. The notion of dressing now arises in the limit $\Omega_1 \ll \Omega_2$ in which the Rydberg population $p_e = (\Omega_1/\Omega_2)^2$ can be made very small despite the resonant Rydberg-state coupling. Consequently, the rate of decoherence due to Rydberg state decay, $p_e\gamma_2$ is strongly suppressed. Our measured atom loss due to Rydberg excitation of a cold strontium gas [Fig. 1(b)] illustrates this suppression around the two-photon resonance, in excellent agreement with the calculated loss rates based on single-atom dynamics.

For larger p_e and densities ρ_a, however, Rydberg-Rydberg atom interactions start to become important. Their major effect is to shift the energy of two excited atoms, as described by the two-body operator $\hat{W}_{ij} = V(r_{ij})\hat{\sigma}_{ee}^{(i)}\hat{\sigma}_{ee}^{(j)}$. For Rydberg states with vanishing orbital angular momentum one can assume isotropic van der Waals interactions, $V = C_6/r_{ij}^6$ that only depend on the interatomic distance $r_{ij} = |\mathbf{r}_i - \mathbf{r}_j|$. The interactions of strontium atoms in $^3S_1$ Rydberg states are repulsive with van der Waals coefficients between $C_6 \sim 9\mu m^6 MHz$ and $700\mu m^6 THz$ for principal quantum numbers $24 < n < 100$ [42]. Thus, the interactions can exceed typical light-matter coupling strengths, $\lesssim 10MHz$, at a large distance of several μm.

While these large energy scales preclude a perturbative treatment in terms of the interaction potential $V(r)$,
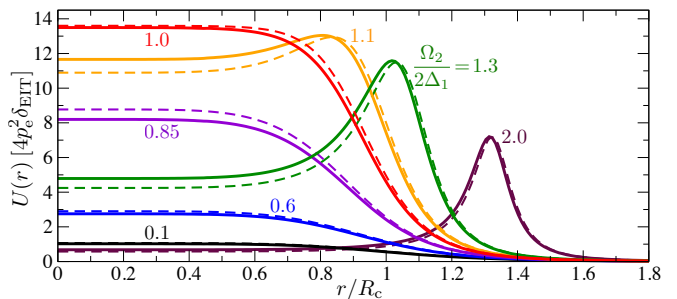

FIG. 2. (color online) Effective interactions for $\Delta_1 + \Delta_2 = 0$, $\Delta_1/\gamma_p = 2.5$, $\Omega_1/\Omega_2 = 0.1$, $\gamma_e = 0$ and different values $\Omega_2/(2\Delta_1)$ as indicated in the figure. The solid lines are obtained from a numerical solution of the two-body Master equation and the dashed lines show the analytical expression eq. (5).

one can derive an approximate Master equation to leading order in the small excitation fraction p_e [43, 44]. To this end we first consider the dynamics of the one-body density matrix

$$\partial_t\hat{\rho}_i^{(1)} = -i\left[\hat{H}_i, \hat{\rho}_i^{(1)}\right] + \mathcal{L}_i(\hat{\rho}_i^{(1)}) - i\sum_{j\neq i}\mathrm{Tr}_j\left[\hat{W}_{ij}, \hat{\rho}_{ij}^{(2)}\right]$$
$$(2)$$

which requires knowledge of the two-body matrices $\hat{\rho}_{ij}^{(2)} = \mathrm{Tr}_{\bar{i},\bar{j}}\hat{\rho}$. Since their evolution

$$\partial_t\hat{\rho}_{ij}^{(2)} = -i\left[\hat{H}_i + \hat{H}_j, \hat{\rho}_{ij}^{(2)}\right] + \mathcal{L}_i(\hat{\rho}_{ij}^{(2)}) + \mathcal{L}_j(\hat{\rho}_{ij}^{(2)})$$
$$- i\left[\hat{W}_{ij}, \hat{\rho}_{ij}^{(2)}\right] - i\sum_{k\neq i,j}\mathrm{Tr}_k\left[\hat{W}_{ik} + \hat{W}_{jk}, \hat{\rho}_{ijk}^{(3)}\right](3)$$

in turn, requires corresponding three-body terms one eventually obtains an infinite hierarchy of equations. The last term in eq. (3), however, involves three excited Rydberg atoms and is effective *only* for mutual distances, $r_{ik}, r_{jk} \lesssim R_c$, below a range R_c of the interaction. The Rydberg excitation number $\varepsilon = p_e R_c^3 \rho_a$ within the interaction volume can, thus, serve as a small parameter. Since $\hat{W}_{ij}$ projects on the doubly excited Rydberg state, the last term is smaller then the direct interaction term, $[\hat{W}_{ij}, \hat{\rho}_{ij}^{(2)}]$, by a factor ε. To leading order in ε, we can, therefore, drop the three-body term and obtain a closed set of equations for the one- and two-body density matrices.

With this simplification the total energy of the system splits into a sum over binary effective interactions

$$U(r_{ij}) = \mathrm{Tr}[\hat{\rho}_{ij}^{(2)}(\hat{H}_i + \hat{H}_j + \hat{W}_{ij})], \qquad (4)$$

and the scattering rate per atom $\Gamma_i = \mathrm{Tr}[\hat{\rho}_i^{(1)}(\gamma_p\hat{\sigma}_{pp}^{(i)} + \gamma_e\hat{\sigma}_{ee}^{(i)})]$ is also influenced by interactions with surrounding particles according to eq. (2).

The effective interaction, $U(r)$, can be straightforwardly obtained by numerically calculating the steady

state of eq. (3) for a pair of atoms driven on two-photon resonance. Fig. 2 illustrates the typical potential form for $\gamma_e = 0$. For $\Omega_2 < \Delta_1$, the potential assumes a soft-core form very similar to those found for Rydberg-dressing of two-level atoms [18, 21]. In contrast to the latter, however, the ratio Ω_2/Δ_1 provides an additional control parameter that enables significant shaping of the potential. In particular, the interaction strength is drastically enhanced as Ω_2 approaches a value of $2\Delta_1$, beyond which it develops a pronounced maximum at finite distances. As shown in Fig. 1(d), the overall strength of the potential is optimized around $\Omega_2 = 2\Delta_1$ regardless of other laser parameters.

A better understanding of this behaviour can be gained from the following analytical solution

$$U(r) - i\Gamma(r) = \tag{5}$$
$$\frac{\Omega_1^4 V}{\Omega_2^4} \frac{4\Delta_1^2 + \gamma_p^2 + 4(4\Delta_1^2 + \gamma_p^2 + \Omega_2^2)(\Delta_1 - i\gamma_p)V/\Omega_2^2}{\left[2\Delta_1 + (4\Delta_1^2 - \Omega_2^2 - \gamma_p^2)\frac{V}{\Omega_2^2}\right]^2 + \gamma_p^2\left(1 + 4\frac{V\Delta_1}{\Omega_2^2}\right)^2}$$

which we derived in the limit $\gamma_p \ll |\Delta_1|$, $\Omega_1 \ll \Omega_2$ and $\Omega_1 \ll \gamma_p$. As shown in Fig. 2, eq. (5) provides an excellent description of the numerical results, with residual deviations stemming from a violation of the last inequality for the chosen parameters.

Expectedly, the interaction scales as $p_e^2 = \Omega_1^4/\Omega_2^4$ since it requires the simultaneous Rydberg excitation of both atoms. Moreover, we can read off the potential range, R_c from the denominator of eq. (5). For $\Omega_2 \ll |\Delta_1|$, R_c follows from $|V(R_c)| = \Omega_2^2/(2|\Delta_1|)$, i.e. is determined by twice the EIT linewidth $\delta_{EIT} = \Omega_2^2/(4|\Delta_1|)$ as also found for effective interactions between photons in Rydberg-EIT media [44, 45]. In the opposite limit, $\Omega_2 > |\Delta_1|$, this energy scale is replaced by $|V(\bar{R}_c)| = 2|\Delta_1|$, such that $\bar{R}_c = (2|\Delta_1|/\Omega_2)^{1/3}$. Again this bears analogies to the behaviour of photonic interactions in such systems [46, 47]. Likewise, eq. (5) yields an interaction strength $U(r \to 0) = 4p_e^2\delta_{EIT}$ for $\Omega_2 \ll |\Delta_1|$, which undergoes a maximum at $\Omega = 2\Delta_1$ where $U_0 = U(r = 0)$ is greatly enhanced by a factor $2\Delta_1^2/\gamma_p^2$ [cf. Fig. 1(d)]. At the same time, the corresponding scattering is suppressed by a factor $|\Delta_1|/\gamma_p$, permitting large interactions to be obtained while ensuring long coherence times.

The origin of this enhancement can be traced back to a two-body resonance that emerges for strong interactions. To this end, consider the coherent laser coupling, which can be expressed in terms of the 6-level scheme shown in Fig. 3(a), where $|\alpha\beta\rangle_+ = (|\alpha\beta\rangle + |\beta\alpha\rangle)/\sqrt{2}$ denote symmetric two-particle states. For $\Omega_2 \gg \Omega_1$, the system approximately separates into three subspaces composed of $|gg\rangle$ and states with one and two excitations, respectively. Fig. 3(b) shows the eigenenergies of the two-excitation subspace. In the limit of large interactions the doubly excited Rydberg state decouples asymptotically and only $|pp\rangle$ and $|pe\rangle_+$ are hybridized by the Rydberg excitation laser. One of the two eigenenergies,
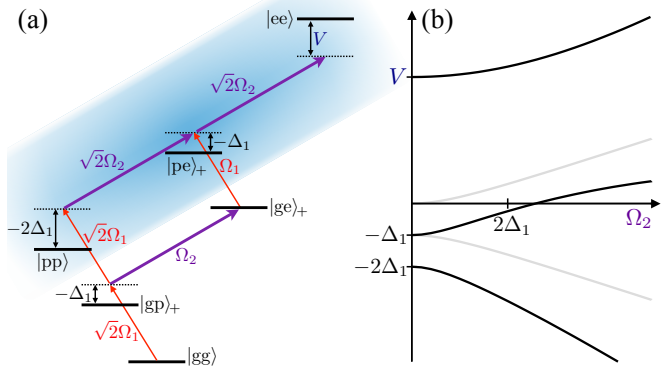

FIG. 3. (color online) (a) Two-body level diagram in terms of atomic pair states on two-photon resonance ($\Delta_1 + \Delta_2 = 0$). (b) The energy spectrum of the doubly excited subspace [black lines and shaded area in (a)] indicates the occurrence of a two-body resonance around $\Omega_2 \approx 2\Delta_1$ that is driven via the singly excited states (grey lines).

$-\frac{3}{2}\Delta_1 \pm \frac{1}{2}\sqrt{\Delta_1^2 + 2\Omega_2^2}$, vanishes at $\Omega_2 = 2\Delta_1$. At this point, the two-atom ground state is coupled resonantly to the corresponding eigenstate $|pp\rangle + \sqrt{2}|pe\rangle_+$ leading to an enhanced light shift. Hence, it is this interaction-induced two-body resonance that enables the enhanced interactions shown in Fig. 1(d) and Fig. 2.

Let us now compare the proposed approach to previous work on Rydberg-dressing of two-level systems [17–21]. There, the underlying three-level atom is simplified to an effective two-level system, driven with a two-photon Rabi frequency $\Omega = \Omega_1\Omega_2/(2\Delta_1)$, assuming $\Omega_1 \ll \Delta_1$. Optical dressing with a large two-photon detuning $\Delta_1 + \Delta_2 = \Delta \gg \Omega$ then yields an effective potential with strength $U_0 = \Omega^4/(2\Delta)^3$ and a scattering rate of $\gamma_p\Omega_1^2/(2\Delta_1)^2 + \gamma_e\Omega^2/(2\Delta)^2$. In Fig. 4 we show the interaction strength U_0 as a function of the Rydberg-excitation Rabi frequency Ω_2 obtained from different dressing schemes for a fixed effective coherence time Γ^{-1}, while optimizing U_0 with respect to all remaining parameters. For strontium atoms, resonant dressing via the $(5s5p)^1P_3$ triplet state ($\gamma_p/(2\pi) = 7.6$kHz) clearly

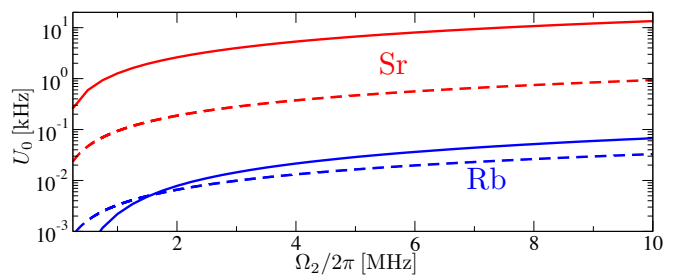

FIG. 4. (color online) Maximum interaction strength at a coherence time $\Gamma^{-1} = 10$ms achievable for Sr (upper two curves) and Rb (lower two curves) atoms from off-resonant dressing (dashed lines) and the approach described in this work (solid).
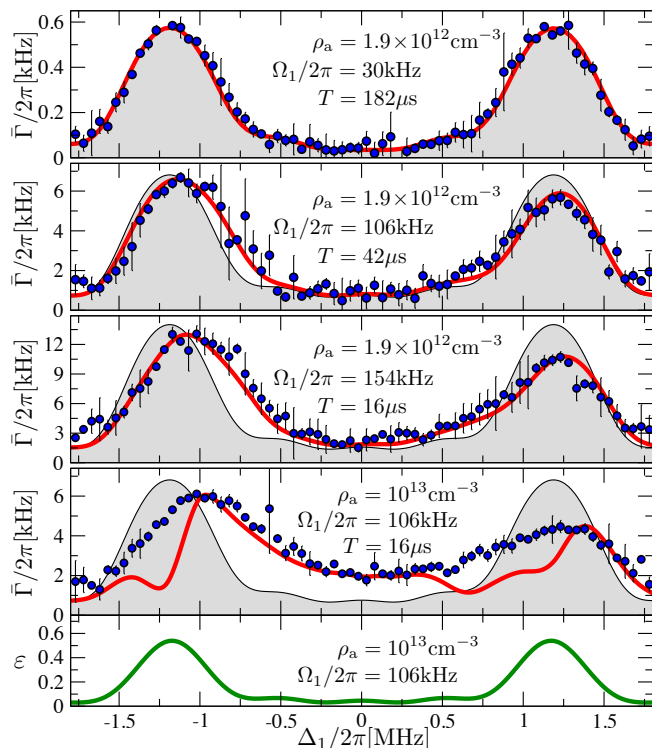
FIG. 5. (color online) Measured (dots) and calculated (lines) loss rates under different conditions indicated in the figure. The shaded areas show the loss spectrum without interactions. The bottom panel shows the parameter ε, indicating the breakdown of the leading-order theory around the Autler-Townes maxima under the indicated conditions. The theory uses $C_6/2\pi = 1.4\mu\mathrm{m}^6\mathrm{MHz}$ [42] and the remaining parameters are given in the text.

outperforms the two-level approach and yields sizeable effective interactions of several kHz, exceeding the scattering rate Γ by up to 2 orders of magnitude. On the contrary, for alkaline atoms, such as Rubidium, both approaches turn out to be rather inefficient due to the large decay rate $\gamma_\mathrm{p}/2\pi = 6.1\mathrm{MHz}$ of the intermediate state, requiring very large Ω_2 in order to realize significant effective interactions. We note that larger interactions can still be obtained from direct single-photon transitions to Rydberg P-states. However, the strong anisotropy of van der Waals interactions between non-zero angular momentum states [48] can lead to pair resonances [28, 35] that cause large losses and render P-state dressing inapplicable in three dimensions. An important feature of our EIT-based approach is that the detrimental effects of such resonances, which can also occur at small distances [22–24, 36] are completely removed. Instead of enhancing the excited Rydberg fraction an occurring pair resonance restores EIT conditions for a dressed atom pair and thereby even enhances the decoherence time instead of suppressing it (see [49] for more details).

We have experimentally investigated the excitation dy-

namics in a cold gas of $^{84}\mathrm{Sr}$ atoms [49]. Details on the cooling and trapping are described in [50]. The atoms are excited to a $(5s24s)^3S_1$ Rydberg state via the long lived $(5s5p)^3P_1$ triplet state with a 689nm and 319nm laser beam with Rabi frequencies Ω_1 and Ω_2, respectively [cf. Fig. 1(a)]. We probe the system by recording atom loss following laser excitation via fluorescence measurements. The gas is excited in a stroboscopic fashion with constant $\Omega_2/2\pi = 2.4\mathrm{MHz}$ while driving the lower transition with a train of $\tau = 2\mu s$ pulses that are separated by $50\mu s$ which is long compared to the Rydberg state lifetime, $\gamma_\mathrm{e}^{-1} \approx 3.8\mu s$ [51]. The number, T/τ, of pulses is chosen such that the total dressing time T yields an accumulated signal well above the noise level of our detection.

Since atom loss has been the major obstacle in previous experiments on Rydberg dressing [52, 53], we have studied losses in our measurements. As $\gamma_\mathrm{e} > \gamma_\mathrm{p}$, the observed atom loss predominantly stems from Rydberg state decay causing photon recoil and transitions to dark intermediate triplet states. Hence, we can estimate the average loss rate $\bar{\Gamma} = N_\ell/(NT)$ from the measured initial (N) and lost (N_ℓ) number of atoms. In order to reach significant losses we chose to work on single-photon resonance ($\Delta_2 = 0$) and record the entire loss spectrum as function of Δ_1. Theoretically, we solve eqs. (2) and (3) for a Gaussian atomic density distribution, accounting for the experimental finite laser linewidths $\gamma_1 = 130\mathrm{kHz}$ and $\gamma_2 = 1.3\mathrm{MHz}$ associated with the lower and upper transition. As described above, dominant binary effective interactions emerge in the limit $\varepsilon \ll 1$, in which we can neglect the three-body terms in eq. (3) to facilitate a numerical solution of eqs. (2) and (3). Fig. 5 shows measured and predicted loss spectra as a function of Δ_1. For our smallest density and Ω_1 the measurement agrees well with the expected single-particle spectrum in the absence of interactions. Upon increasing Ω_1 we observe clear density effects caused by Rydberg-Rydberg atom interactions. As shown in Fig. 5, this leads to larger losses around the two-photon resonance, $\Delta_1 = 0$, and a growing asymmetry of the two Autler-Townes maxima around $\Delta_1 = \pm\Omega_2/2$. We observe up to fourfold changes of the loss rate by the interactions that are remarkably well by the theory provided $\varepsilon \ll 1$. At the same time, the deviations outside of this regime indicate the emergence of higher order effective interactions between the Rydberg-dressed atoms.

In conclusion, we have developed an approach to generate finite-range atomic interactions via two-photon resonant optical coupling to Rydberg states. This system entails interesting physics, such as an interaction-induced two-body resonance that leads to enhanced effective interactions while preserving long coherence times. Moreover, the possibility to engineer atomic interactions under Rydberg-EIT conditions [54] opens up new perspectives, e.g. concerning the coupled nonlinear dynamics of light [44] and matter wave fields, which

mutually induce effective interactions for either component based on the mechanism discussed in this work. The enhanced interactions together with the demonstrated immunity to short-distance pair-resonances holds promise for studying finite-range interactions in quantum gases. Our loss measurements provide the first demonstration of strong interactions in a cold gas of triplet Rydberg states. The good agreement with the theoretical picture of dressing-induced effective interactions supports the promise of the new dressing-approach developed in this work. For longer excitation times, τ, our measurements suggest the presence of an additional loss mechanism [55] that most likely stems from dipolar interactions with P-state Rydberg atoms produced by black-body radiation [53]. The developed theoretical framework appears suitable for studying this problem and exploring potential solutions. The promising results of this work motivate future experiments to address this issue and realize narrow-bandwidth dressing off single-photon resonance ($\Delta_1 \neq 0$) to generate and probe coherent interactions in atomic quantum gases.

[1] I. Bloch, J. Dalibard and W. Zwerger, Rev. Mod. Phys. **80**, 885 (2008).
[2] J. Deiglmayr *et al.*, Phys. Rev. Lett. **101**, 133004 (2008).
[3] K.-K. Ni *et al.*, Science **322**, 231 (2008).
[4] S. A. Moses *et al.*, Science **350**, 659 (2015).
[5] A. Griesmaier *et al.*, Phys. Rev. Lett. **94** 160401 (2005).
[6] M. Lu *et al.*, Phys. Rev. Lett. **107** 190401 (2011).
[7] H. Kadau *et al.*, arXiv:1508.05007
[8] B. P. Lanyon *et al.*, Science **334**, 57 (2011).
[9] R. Islam *et al.*, Nature Commun. **2**, 377 (2011).
[10] C. Senko *et al.*, Phys. Rev. X **5**, 021026 (2015).
[11] P. Jurcevic *et al.*, Phys. Rev. Lett. **115**, 100501 (2015).
[12] M. Saffman, T. G. Walker and K. Mølmer, Rev. Mod. Phys. **82**, 2313 (2010).
[13] P. Schauß *et al.*, Nature **491**, 87 (2012).
[14] P. Schauß *et al.*, Science **347**, 1455 (2015).
[15] D. Barredo *et al.*, Phys. Rev. Lett. **114**, 113002 (2015).
[16] H. Labuhn *et al.*, arXiv:1509.04543
[17] I. Bouchoule and K. Mølmer, Phys. Rev. A **65**, 041803(R) (2002).
[18] N. Henkel, R. Nath and T. Pohl, Phys. Rev. Lett. **104**, 195302 (2010).
[19] G. Pupillo *et al.*, Phys. Rev. Lett. **104**, 223002 (2010).
[20] J. Honer *et al.*, Phys. Rev. Lett. **105**, 160404 (2010).
[21] J. E. Johnson and S. L. Rolston, Phys. Rev. A **82**, 033412 (2010).
[22] Y.-Y. Jau *et al.*, Nature Phys. **12**, 17 (2016).
[23] T. Keating *et al.*, Phys. Rev. A **87**, 052314 (2013).
[24] T. Keating *et al.*, Phys. Rev. A **91**, 012337 (2015).
[25] S. Möbius *et al.*, Phys. Rev. A 87, 051602(R) (2013).
[26] L. I. R. Gil *et al.*, Phys. Rev. Lett. **112**, 103601 (2014).
[27] F. Cinti *et al.*, Phys. Rev. Lett. 105, 135301 (2010).
[28] F. Maucher *et al.*, Phys. Rev. Lett. 106, 170401 (2011).
[29] N. Henkel *et al.*, Phys. Rev. Lett. **108**, 265301 (2012).
[30] A. Dauphin, M. Müller, and M. A. Martin-Delgado, Phys. Rev. A **86**, 053618 (2012).
[31] F. Cinti *et al.*, Nature Comm. **5**, 3235 (2014).
[32] X. Li and S. Das Sarma, Nature Comm. **6**, 7137 (2015).
[33] A. Geißler, I. Vasic, W. Hofstetter, arXiv:1509.06292
[34] A.W. Glaetzle *et al.*, Phys. Rev. X **4**, 041037 (2014).
[35] A. W. Glaetzle *et al.*, Phys. Rev. Lett. **114**, 173002 (2015).
[36] R.M.W. van Bijnen and T. Pohl, Phys. Rev. Lett. **114**, 243002 (2015).
[37] J. Millen, G. Lochead, and M. P. A. Jones, Phys. Rev. Lett. **105**, 213004 (2010).
[38] P. McQuillen *et al.*, Phys. Rev. A **87**, 013407 (2013).
[39] G. Lochead *et al.*, Phys. Rev. A **87**, 053409 (2013).
[40] B. J. DeSalvo *et al.*, Phys. Rev. A **92**, 031403 (2015).
[41] M. Fleischhauer, A. Imamoglu, and J. P. Marangos, Rev. Mod. Phys. **77**, 633 (2005).
[42] C. L. Vaillant, M. P. A. Jones, R. M. Potvliege , J. Phys. B **45** 135004 (2012).
[43] H. Schempp *et al.*, Phys. Rev. Lett. **104**, 173602 (2010).
[44] S. Sevincli *et al.*, Phys. Rev. Lett. **107**, 153001 (2011).
[45] A. V. Gorshkov *et al.*, Phys. Rev. Lett. **107**, 133602 (2011).
[46] T. Peyronel *et al.*, Nature **488**, 57 (2012).
[47] P. Bienias *et al.*, Phys. Rev. A **90**, 053804 (2014).
[48] T. G. Walker and M. Saffman, Phys. Rev. A **77**, 032723 (2008).
[49] See Supplemental Material at [URL] for further details of our experiments as well as more details and explicit calculations on the effects of additional pair-resonances.
[50] Y. N. Martinez de Escobar *et al.*, Phys. Rev. Lett. **103**, 200402 (2009).
[51] S. Kunze *et al.*, Z. Phys. D **27**, 111 (1993).
[52] J. B. Balewski *et al.*, New J. Phys. **16**, 063012 (2014).
[53] E. A. Goldschmidt *et al.*, arXiv:1510.08710
[54] J. D. Pritchard *et al.*, Phys. Rev. Lett. **105**, 193603 (2010).
[55] B. J. DeSalvo *et al.*, arXiv:1510.08032
[56] S. Helmrich *et al.*, arXiv:1510.09057